Chemical Engineering Journal 146 (2009) 388–400

Contents lists available at ScienceDirect

Chemical Engineering Journal

journal homepage: www.elsevier.com/locate/cej

Prediction of SO_2 and NO_x emissions for low-grade Turkish lignites in CFB combustors

Afsin Gungor*

Department of Mechanical Engineering, Faculty of Engineering and Architecture, Nigde University, 51100 Nigde, Turkey

ARTICLE INFO

Article history:
Received 15 March 2007
Received in revised form 1 June 2008
Accepted 21 June 2008

Keywords:
Circulating fluidized bed
Modeling
Coal combustion
SO_2 emission
NO_x emission

ABSTRACT

The CFB technology is widely used for combustion of coal because of its unique ability to handle low quality, high ash, high sulphur and low heating value coals. This paper presents a modeling study of pollutant emissions such as sulphur dioxide (SO_2) and nitric oxide (NO_x) resulting from coal combustion in a CFBC. Using this model, overall SO_2 and NO_x emissions are predicted for the combustion of three different kinds of low-grade Turkish lignites. The contents of these lignites are as follows: ash from 23.70% to 45.31%, sulphur from 1.81% to 8.40% and calorific values (LHV) from 10,283 to 15,215 kJ/kg. The data is obtained from two pilot scale CFBCs (50 and 80 kW) and an industrial scale CFBC (160 MW). The present study proves that CFB combustion demonstrated by both experimental data and model predictions produces low and acceptable level of SO_2 and NO_x emissions resulting from the combustion of low-grade lignites. Developed model can also investigate the effects of different operational parameters on overall SO_2 and NO_x emissions. As a result of this investigation, it is observed that increase of excess air decreases SO_2 and NO_x emissions. However, NO_x emission increases with the operational bed velocity while SO_2 emission decreases. A bigger inlet bed pressure value results in lower emissions of SO_2 and NO_x if other parameters are kept unchanged.

1. Introduction

The use of fossil fuels in an energy production system should be considered with its adverse effects on the environment. While the energy consumption in the world increases gradually, pollutant gases in atmosphere also increase. Because of that reason, there are many studies in the literature using coal in energy production to supply increasing energy demand as well as to minimize environmental pollution. An appropriate technology must be employed to avoid the production of pollutants and other problems while maximizing process efficiency [1–3].

CFB combustion is receiving wide research attention in view its potential as an economic and environmentally acceptable technology for burning low-grade coals. In addition to highly efficient operation, a combustion system should comply with the requirement of minimizing environmental impact. The emission rate of various pollutants from the combustion of coal depends on fuel analysis, combustor design and operating conditions. Fluidized bed combustion allows clean and efficient combustion of coal. Designing of the CFB combustor (CFBC) is very important because of burning coal with high efficiency and within acceptable levels of gaseous emissions. A good understanding of the combustion and pollutant generating processes in the combustor can greatly avoid costly upsets. One of the major advantages of CFBCs is their efficiency for combustion of low-grade lignites [2,4,5].

For the reduction of pollutant emissions from coal-fired power plants, numerous techniques, involving the staged input of fuel and air have been successfully applied. The application of these techniques to industrial scale combustors necessitates combustion parameters optimization that is extremely time-consuming and expensive. Mathematical modeling allows the testing of many variable combustion parameters in a much shorter time period and at lower costs. Therefore, mathematical modeling application in the CFB combustion process to enhance combustion performance and reduce pollutants is seen as an attractive solution. Investigations about the CFB modeling have been carried out by many different researchers in the literature [1,3,6–15].

A detailed review of studies concerning CFB combustion and their modeling has been presented by Reh [2] who argues that there must be a balance between the computational modeling and verification by experimental and operational results. It is claimed that there has to be a cooperation between the plant designers–operators and the academia to provide a reliable basis of experimental data. The most important demands to be considered

* Tel.: +90 532 397 30 88; fax: +90 388 225 01 12.
E-mail address: afsingungor@hotmail.com.

1385-8947/$ – see front matter © 2008 Elsevier B.V. All rights reserved.
doi:10.1016/j.cej.2008.06.019

Nomenclature

Ar	Archimedes number
C	gas concentration (kmol/m^3)
Ca/S	calcium to sulphur ratio
c	specific heat (kJ/kg K)
D	bed diameter (m)
D_b	Equivalent bubble diameter (m)
D_g	diffusivity coefficient for oxygen in nitrogen (m^2/s)
d	diameter (m)
d_p	particle diameter (m)
d_{pi}	particle dimension interval (m)
EA	excess air
e	emissivity
g	gravity (m/s^2)
H_b	combustor height (m)
h	overall bed to wall heat transfer coefficient (W/m^2 K)
h_g	convection heat transfer coefficient for gas phase (W/m^2 K)
h_p	convection heat transfer coefficient for particle phase (W/m^2 K)
h_r	radiative heat transfer coefficient (W/m^2 K)
k	rate constant (m/s)
k_a	attrition constant
k_{be}	mass transfer coefficient (1/s)
k_c	char combustion reaction rate (kg/s)
k_f	fragmentation coefficient
k_g	gas conduction heat transfer coefficient (W/m/K)
k_L	reaction rate (1/s)
k_{vL}	volumetric reaction rate (kg/m^2 s)
$\dot{m}$	mass flow rate (kg/s)
m_f	feed rate (kg/h)
$\dot{n}$	gas flow rate (mol/s)
$P(f)$	particle size distribution function on a mass basis of the fragments (1/m)
Pr	Prandtl number
R	reaction rate (mol/s, mol/cm^3 s)
R_b	bed radius (m)
R_g	gas constant (kJ/mol K)
r	radial distance from riser axis (m)
r_{mother}	radius of the mother particle (m)
S_g	specific surface area of limestone particles (m^2/kg)
Sh	Sherwood number
T	temperature (K)
T_{mean}	mean bed temperature (K)
U_0	superficial velocity (m/s)
U_{mf}	minimum fluidization velocity (m/s)
U_{ter}	terminal velocity (m/s)
u	gas velocity (m/s)
V	volatile yield
v	particle velocity (m/s)
X_k	char mass fraction, kg-char/(kg-bed material)
x_a	weight fraction of particles after attrition at d_{pi} interval

Subscripts

ash	ash
b	bed
burn	burn
c	carbon
e	emission
g	gas
p	particle
s	solid
wall	wall

Greek letters

$\Delta\dot{m}_C$	carbon mass flow rate consumed from physical/chemical process (kg/s)
$\Delta\dot{n}$	gas flow rate consumed from chemical processes (kmol/s)
ΔV	volume of the cell (m^3)
β'	constant defined in Eq. (8)
ε	void fraction
ε_b	bubble volume fraction
λ_s	limestone reactivity
ρ	particle density (kg/m^3)
σ	Stefan–Boltzman coefficient (W/m^2 K^4)

for future efforts in research, design and operation of CFBC are to improve multi-scale two-phase modeling in direction of the improvement of validation using CFB data bases. The improved mastery of CFBC design basics as a gas–solid reactor is still essential [16].

Basu [1] presented a comprehensive review of combustion of coal in CFBs. In that study coal combustion models are grouped under three levels of details of sophistication: *Level I*: The simplest model is 1D with plug flow reactor, where solids are back-mixed [6,7]. The 1D models do not consider the solid flow in the annular region of the riser, where temperature, gas concentration and velocity can differ from that in the core, in which an upflowing dilute region is considered. *Level II*: Core-annulus, 1.5D, with broad consideration of combustion and other related processes [8–12]. *Level III*: 3D model based on Navier Stokes equation [13–15].

Numerous experimental and theoretical studies about gaseous emissions in CFBCs are present in the literature [4,9,14–37]. Nitrogen oxides are a major environmental pollutant resulting from combustion. The reactions of nitrogen oxides with carbons or chars are of current interest with regard to their possible role in reducing NO_x emissions from combustion systems. They also offer new useful insights into the oxidation reactions of carbons, generally [17]. A large literature concerning these reactions has developed, as evidenced in three reviews [18–20] and by the recent publication of many papers in the area [4,15–24,26,29,30,34]. These works have suggested considerable complexity in the mechanisms of NO_x reduction and a large variability in reported kinetics. There are two approaches to describe NO_x emission in CFB [26]. The first approach involves overall reaction (considering catalytic activity of CaO and char). The overall rate constants are measured preferably under CFB conditions [27]. The other approach is more thorough, and is based on actual chemical reactions whose rate constants can be taken from literature [28]. For CFB only 106 reactions with 28 species were used to model the NO_x emission. However, a detailed review shows that all N-related reactions have not the same importance [29]. So instead of considering all N-related reactions, one could use only the important reactions for the development of a predictive procedure for the overall NO_x emission from a CFBC.

Reducing SO_2 emission from power plants is one of the main issues for the environmental protection. One of the advantages of the circulating fluidized bed combustion technology of coal is in situ SO_2 capture by added sorbents, usually uncalcined limestone ($CaCO_3$). Numerous experimental and theoretical studies

about the sulphur retention in CFBCs are present in the literature [4,9,15,25,31–37]. Some models have already been proposed for predicting the sulphur retention in CFBC, but there are important differences between their sub-models, especially as far as the CFB hydrodynamics is considered [4,15,31].

Because coal combustion in a CFB combustor directly is affected by its hydrodynamic parameters, both hydrodynamic and combustion models are treated simultaneously to yield a predictive model for the CFB combustor. It has been widely accepted that a CFB combustor may be characterized by two flow regimes: a dense bed at the bottom and a dilute region above the secondary air inlet. There are great differences in the hydrodynamics between the dense bed and the dilute region. However, most of the models in the literature do not completely take account of the performance of the dense bed, consider the dense bed as well-mixed distributed flow with constant voidage, and use generally lumped formulation [3,7–15,17–32,38]. Experimental evidence has been reported by Svensson et al. [39], and Werther and Wein [40] that, the fluid dynamical behavior of the dense bed is similar to that of bubbling fluidized beds. Furthermore, the results of studies of Leckner et al. [41] and Montat and Maggio [42] imply that the combustion of coal, particles mixing and heat transfer in the dense bed dominate the performances of CFB. This implies that, bottom zone should be modeled in detail as two-phase flow. However, most of the models in the literature do not completely take account of the performance of the bottom zone, consider the bottom zone as well-mixed distributed flow with constant voidage, and use generally lumped formulation [3,7–15,17–32]. In the present study, the bottom zone is modeled in detail as two-phase flow which is subdivided into a solid-free bubble phase and a solid-laden emulsion phase [8,41,42] which constitutes a difference from the previous studies in the literature. Furthermore, the present model integrates and simultaneously predicts the hydrodynamics, heat transfer and combustion aspects.

The objective of the model presented in this study is to be able to predict the pollutant emissions formation and destruction of different low-grade Turkish lignites in various sizes of CFBCs. There are considerable reserves of lignite in Turkey. Most of Turkish lignite reserves are of low-grade lignites with a calorific value of about 12,000 kJ/kg, ash content of about 25–30% and average sulphur content of about <4%. The main problem for Turkish units running on lignite is presented by the air emissions [43].

This paper presents a modeling study of pollutant emissions such as SO_2 and NO_x resulting from coal combustion in a CFBC. Using this model, overall SO_2 and NO_x emissions are predicted for the combustion of three different kinds of low-grade Turkish lignites. The contents of these lignites are as follows: ash from 23.70% to 45.31%, sulphur from 1.81% to 8.40% and calorific values (LHV) from 10,283 to 15,215 kJ/kg. The data is obtained from two pilot scale CFBCs (50 and 80 kW) and an industrial scale CFBC (160 MW). Developed model can also investigate the effects of different operational parameters on overall SO_2 and NO_x emissions.

In the model, the CFB riser is analyzed in two regions: The bottom zone is modeled in detail as two-phase flow. In the upper zone core-annulus solids flow structure is established. Kinetics of char combustion is modeled with a shrinking core model with mixed control by chemical reaction and gas film diffusion, assuming that the ash separated once formed. The particle size distribution due to fuel particle fragmentation, char combustion and particle attrition is also considered. The volatiles are released in emulsion phase in the bottom zone at a rate proportional to the solid mixing rate. Model calculates the axial and radial distribution of voidage, velocity, particle size distribution, pressure drop, gas emissions and temperature at each time interval for gas and solid phase both for bottom and upper zones.

2. Model description

The use of CFB modeling enables the analysis of a combustion system involving fluid flow, heat transfer, and combustion and pollutant emissions. The two-phase fluid dynamics is of great importance for the design and operation of the CFBCs [2]. Because of containing complex gas–solid flow and gas phase reactions, modeling of CFBCs is rather difficult. The fluid dynamics of this gas–solid two-phase flow is very complex and strongly dominated by particle-to-particle interactions. Furthermore, the numerous homogeneous and heterogeneous catalytic gas phase reactions and their kinetics for the description of the combustion phenomena and the emission formation and destruction are not completely known. Therefore, it is necessary to develop simplified modeling approaches, which can describe both the gas–solid flow structure and the combustion process with sufficient accuracy. The main goal of the modeling of CFBCs is to constitute a system that maximizes combustion efficiency, and minimizes operating and investment costs and air pollutant emissions.

Based on previous work on dynamic 2D coal combustion modeling of CFBCs [34], a modeling study of pollutant emissions resulting from coal combustion in CFBCs is present in this study. The present CFBC model can be divided into three major parts: a sub-model of the gas–solid flow structure; a reaction kinetic model for local combustion and a convection/dispersion model with reaction. The latter formulates the mass balances for the gaseous species and the char at each control volume in the flow domain. Kinetic information for the reactions is supplied by the reaction kinetic sub-model, which contains description of devolatilization and char combustion, and emission formation and destruction, respectively.

2.1. Hydrodynamics structure

Combustor hydrodynamic is modeled taking into account previous work [44]. According to the axial solid volume concentration profile, the combustor riser is axially divided into two different zones: The bottom zone is located between distributor plate and secondary air supply and the upper zone is located between secondary air supply and riser exit.

2.1.1. Bottom zone

As mentioned above, most of the models in the literature do not completely take account of the performance of the dense bed, consider the dense bed as well-mixed distributed flow with constant voidage, and use generally lumped formulation [3,7–15,17–32]. In this study, the bottom zone is modeled in detail as two-phase flow.

In the literature, Leckner et al. [41], Palchonock et al. [45] and Huilin et al. [46] claim that this zone could be explained by the presence of bubble-like voids that characterizes the gas flow. On the other hand, it is not clear whether the bed is more behaving as a bubbling fluidized bed or is in the turbulent fluidization regime. Schlichthaerle and Werther [47] are concluded that in the core region turbulent fluidization is more probable whereas the wall region is rather a dense bubbling fluidized bed. Werther and Wein [40] described the expansion behavior of the turbulent CFB bottom zone by a model that is based on modified equations which were originally developed for conventional bubbling fluidized beds. These results lead to the conclusion that in the bottom zone of CFB reactors another two-phase flow structure is established with a solid-rare bubble phase and a solid-laden emulsion phase. In the model, the flow domain is subdivided into n control volumes that each one has a solid-rare bubble phase and a solid-laden emulsion phase. The bubble rise velocity, the bubble volume fraction and the

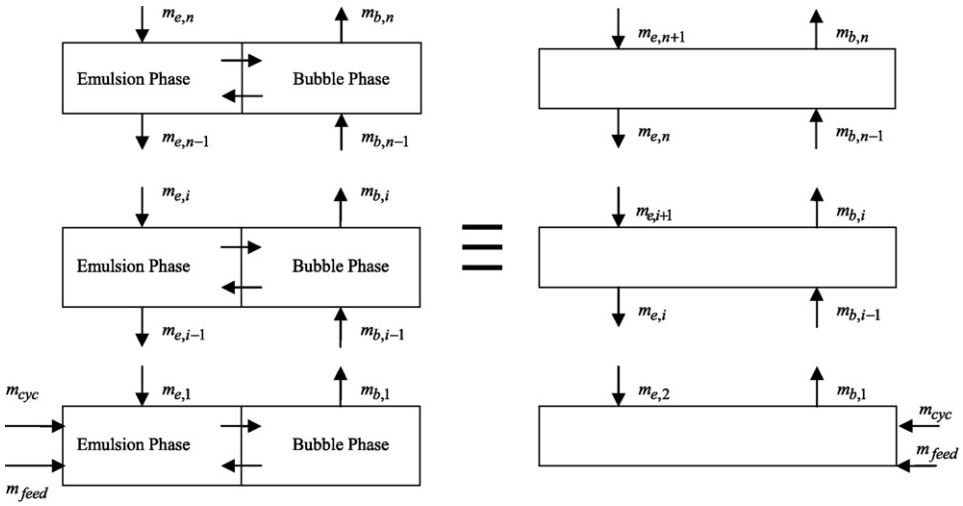

Fig. 1. A single-phase back-flow cell model.

suspension porosity is calculated by Horio [48] as follows:

$$\varepsilon_b = \frac{\dot{V}_b}{u_b} \tag{1}$$

$$\dot{V}_b = \varphi(U_0 - U_{mf}) \quad (\varphi = 1.45Ar^{-0.18},\ 10^2 < Ar < 10^4) \tag{2}$$

$$u_b = \dot{V}_b + \gamma\sqrt{gD_b} \tag{3}$$

$$\frac{\gamma}{0.71} = \begin{cases} 0.63 & (D < 0.1\,\text{m}) \\ 2.0\sqrt{D} & (0.1\,\text{m} < D \le 1.0\,\text{m}) \\ 2.0 & (1.0\,\text{m} < D) \end{cases} \tag{4}$$

where D_b is the bubble diameter [49] and U_{mf} is the minimum fluidization velocity [50]. A single-phase back-flow cell model is used to represent the solid mixing in the bottom zone. The overall material balance for the solids in the ith control volume, in terms of the backmix flow (Fig. 1) in emulsion and bubble phases, $\dot{m}_{e,i}$ and $\dot{m}_{b,i}$ is given by the following equation:

$$\left(\frac{dm}{dt}\right)_i = \dot{m}_{b,i-1} - \dot{m}_{b,i} + \dot{m}_{e,i+1} - \dot{m}_{e,i} - \dot{m}_{burn,i} + \dot{m}_{ash,i} \tag{5}$$

A two-phase model is used for gas phase material balance (Fig. 2). The material balance for the gas phase in the ith control volume for emulsion and bubble phases are given below, respectively:

$$\left(\frac{dn_k}{dt}\right)_{e,i} = \dot{n}_{e,k,i-1} - \dot{n}_{e,k,i} - k_{be}\ \Delta V_i \varepsilon_{b,i}(C_{e,k,i} - C_{b,k,i}) + \Delta\dot{n}_{e,k,i} \tag{6}$$

$$\left(\frac{dn_k}{dt}\right)_{b,i} = \dot{n}_{b,k,i-1} - \dot{n}_{b,k,i} + k_{be}\ \Delta V_i \varepsilon_{b,i}(C_{e,k,i} - C_{b,k,i}) + \Delta\dot{n}_{b,k,i} \tag{7}$$

where $\dot{n}_k$ indicates the gas flow rate of gas components (volatile gases, O_2, CO, CO_2, SO_2, NO_x, and water vapor in the emulsion phase and O_2, CO_2, SO_2, and NO_x in the bubble phase, respectively), V_i is the volume of the ith control volume. The interchange coefficient, k_{be}, between the bubble and the emulsion phases is a function of the bubble diameter and varies along the axis of the bottom zone and is calculated by Rajan and Wen [51].

2.1.2. Upper zone

Core-annulus flow structure is used for the upper zone [52]. Thickness of the annulus varies according to the bed height [40]. A mathematical expression proposed by Smolders and Baeyens [52] for describing the characteristic S-shaped voidage distribution is used to predict the bed density in the model. Solid volume fraction has an approximately parabolic form and is considered as follows [53]:

$$\frac{\varepsilon_p}{\bar{\varepsilon}_p} = 1 - \frac{\beta'}{2} + \beta'\left(\frac{r}{R_b}\right)^2 \tag{8}$$

where the value of β' falls in the range of $1.3 \le \beta' \le 1.9$ and β' increases with increasing superficial gas velocity and decreasing riser diameter [53]. β' value is taken as 1.3 in the model calculations which statically best fits to the experimental data for small-scale CFBCs [43]. The pressure drop through the bottom zone is equal to

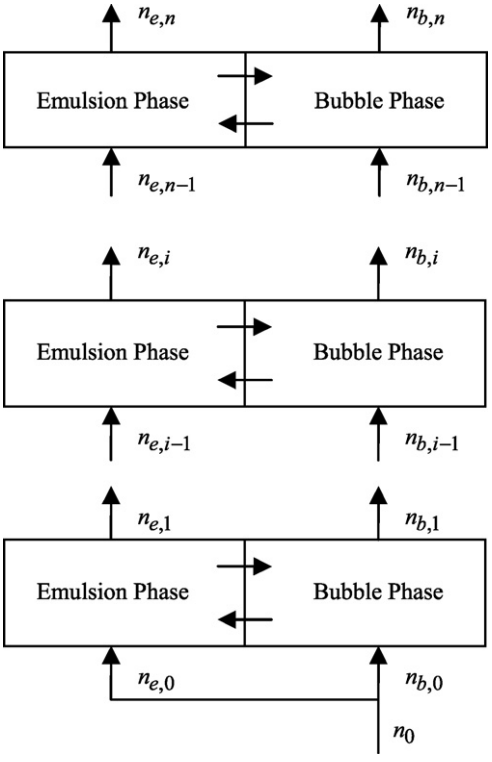

Fig. 2. Two-phase model for the gas phase.

the weight of the solids in this region and considered only in axial direction.

In the upper zone, pressure drop due to the hydrodynamic head of solids is considered in axial direction while having determined the voidage and velocity profiles of solids, pressure drop due to solids acceleration is also considered in axial and radial directions.

Developed hydrodynamic model in the previous work [44] takes into account the axial and radial distribution of voidage, velocity and pressure drop for gas and solid phase, and solids volume fraction and particle size distribution for solid phase. The model results are compared with and validated against atmospheric cold bed CFB units' experimental data given in the literature for axial and radial distribution of void fraction, solids volume fraction and particle velocity, total pressure drop along the bed height and radial solids flux. Ranges of experimental data used in comparisons are as follows: bed diameter from 0.05 to 0.418 m, bed height from 5 to 18 m, mean particle diameter from 67 to 520 μm, particle density from 1398 to 2620 kg/m^3, mass fluxes from 21.3 to 300 kg/m^2 s and gas superficial velocities from 2.52 to 9.1 m/s.

2.2. Kinetic model

The combustor model takes into account the devolatilization of coal, and subsequent combustion of volatiles followed by residual char. As a result of the experimental studies carried out using various types of Turkish lignite, it is known that volatilization products enter the upper region in fluid beds working at slower rates than CFBs [54–56]. Experiments with CFBs give the same results. Therefore, the transition of these products should be taken into consideration in modeling. In the model, volatiles are entering the combustor with the fed coal particles. It is assumed that the volatiles are released in emulsion phase in the bottom zone of the CFBC at a rate proportional to the solid mixing rate. The degree of devolatilization and its rate increase with increasing temperature. The composition of the products of devolatilization in weight fractions is estimated from the correlations proposed by Loison and Chauvin [57].

The bed material in the combustor consists of coal, inert particles and limestone. The properties and size distribution of particles have significant influence on the hydrodynamics and combustion behavior in the CFBC [10]. The model also considers the particle size distribution due to fuel particle fragmentation [58,59], char combustion [11] and particle attrition [60]. Particles in the model are divided into 10 size groups in the model. The Sauter mean diameter is adopted as average particle size. Particles in the bottom zone include particles coming from the solid feed and re-circulated particles from the separator.

In CFBCs, fragmentation of coal particles in a fluidized bed occur within a few seconds after injection of the particles into the bed due to build-up of thermal and devolatilization-induced stresses [58,59]. In the model, the effects of particle fragmentation are taken into account in terms of a fragmentation constant (k_f), and a distribution function (P_f) of fragments, where fragmentation constant is considered as follows [61]:

$$k_f = \frac{3.25 \times 10^{-6}}{r_{mother}} \tag{9}$$

Kinetics of char combustion is modeled with a shrinking core with attiring shell, i.e. the dual shrinking core model (assuming that the ash separated once formed) with mixed control by chemical reaction and gas film diffusion. The rate at which particles of size r_i shrink as follows [11]:

$$r(r_i) = -\frac{dr_i}{dr} = \frac{12C_{O_2}}{\rho X_{k,i}(1/k_{c,i} + d_{p,i}/Sh_i D_g)} \tag{10}$$

The term C_{O_2} indicates the effective oxygen concentration seen by the char particles burning at any point of the combustion chamber. The kinetic constants for the different kinds of low-grade Turkish lignites used in the model are determined by [54–56].

Weight fraction of particles after attrition is considered as follows:

$$x_a = \frac{k_a(u-v)}{d_{pi}} \tag{11}$$

where k_a is the attrition constant and is obtained varying in the range 2–7 × 10^{-7} with a superficial gas velocity of 4–6 m/s and a circulating solids mass flux from 100 to 200 kg/m^{2}s [10]. In the model, the attrition constant value is taken as 2 × 10^{-7} for the coal particles in the model calculations in both bottom zone and upper zone and the attrition constant value of the coal ash particles is taken as 1.7 × 10^{-7} [54,55].

2.2.1. SO_2 emission

Oxides of sulphur produced in burning the coal may be retained in solid form by reaction with particles of limestone or dolomite which is directly fed to the CFBC together with the solid fuel. At the combustion temperatures, usually in the range of 800–900 °C, the $CaCO_3$ calcines to CaO and CO_2. The porous alkaline solid, CaO, produced by the calcination of limestone reacts with SO_2:

$$CaO + SO_2 + \tfrac{1}{2}O_2 \rightarrow CaSO_4 \tag{12}$$

Based on the stoichiometry of the sulphur capture reaction with calcium oxide, a theoretical limestone feed of one mole calcium per mole of sulphur would be enough for complete sulphur capture. However, the molar volume of the reaction product $CaSO_4$ is about three times greater than the molar volume of CaO, therefore complete conversion of the adsorbent particle is impossible, because sulphation only proceeds at the outer shell of the CaO particle [62] and formation of $CaSO_4$ causes pore mouth closure and reaction stops before all the CaO is consumed by the reaction [63]. This sulphation pattern is commonly referred to as the unreacted-core model [64–66]. The Ca utilization of limestone is known to be highly dependent on the flue gas temperature and particle size. Several researchers have found that increasing particle size reduces the utilization significantly, and that the sulphur capture capacity passes through a maximum at temperatures between about 800 and 850 °C [67–69]. As a result, Ca/S mole ratio is usually chosen between two and four in a classical fluidized bed combustor [70]. On the other hand, high SO_2 retention efficiencies were obtained for Ca/S mole ratios of less than two in a circulating fluidized bed combustor [71].

In CFBC the SO_2 generation and retention processes take place simultaneously in the bed [61]. In the model, it is also assumed that the particle size of limestone particles change during the sulphation reaction and the attrition of limestone particles are taken into account. Moreover, the estimation of limestone particles is assumed instantaneous. The chemical reactions with their corresponding reaction rate for SO_2 retention regarding the gas temperature and particle size are given in Table 1.

2.2.2. NO_x emission

It was shown in the literature that [74,75] rather low NO_x emissions are obtained by staged combustion in a fluidized bed combustor. By the use of primary and secondary air injected at different locations in a circulating fluidized bed combustor, its temperature and combustion atmosphere is well-regulated and generally low NO_x emissions of about 150–350 ppm are reported [76].

It is crucial to well evaluate the mechanism of NO_x formation to reduce NO_x in the combustor. However, the mechanism of NO_x

Table 1
The reactions and reaction rates used in the model

Reaction	Reaction rate	
$HCN + \frac{1}{2}O_2 \rightarrow CNO$	$k = 2.14 \times 10^5 \exp\left(\frac{-10000}{T}\right)$	$R_{HCN} = kC_{O_2}C_{HCN}(mol/m^3\,s)$ [80]
$CNO + \frac{1}{2}O_2 \rightarrow NO + CO$	$\frac{k_2}{k_1} = 1.02 \times 10^9 \exp\left(\frac{-25460}{T}\right)$	$R_{CNO-O_2} = kC_{O_2}C_{HCN}\left(\frac{k_1}{k_1+k_2C_{NO}}\right)$ $(mol/m^3\,s)$ [80]
$CNO + NO \rightarrow N_2O + CO$	$k = 2.14 \times 10^5 \exp\left(\frac{-10000}{T}\right)$	$R_{CNO\text{-}NO} = kC_{O_2}C_{HCN}\left(\frac{k_2C_{NO}}{k_1+k_2C_{NO}}\right)$ $(mol/m^3\,s)$ [80]
$N_2O + C \rightarrow N_2 + CO$	$k = 2.9 \times 10^9 \exp\left(\frac{-16983}{T}\right)$	$R_{N_2OC} = kN\pi d_c^2 C_{N_2O}$ (mol/s) [24]
$N_2O + CO \rightarrow N_2 + CO_2$	$k = 5.01 \times 10^{13} \exp\left(\frac{-4.40\times10^4}{R_uT}\right)$	$R_{N_2O-CO} = kC_{N_2O}C_{CO}$ $(mol/cm^3\,s)$ [24]
$N_2O + \frac{1}{2}O_2 \rightarrow N_2 + O_2$	$k = 1.00 \times 10^{14} \exp\left(\frac{-2.80\times10^4}{R_uT}\right)$	$R_{N_2O-O_2} = kC_{N_2O}C_{O_2}$ $(mol/cm^3 s)$ [24]
$NO + C \rightarrow \frac{1}{2}N_2 + CO$	$k = 5.85 \times 10^7 \exp\left(\frac{-12000}{T}\right)$	$R_{NOC} = kN\pi d_c^2 C_{NO}$ (mol/s) [80]
$NO + \frac{1}{2}C \rightarrow \frac{1}{2}N_2 + \frac{1}{2}CO_2$	$k = 1.3 \times 10^5 \exp\left(\frac{-17111}{T}\right)$	$R_{2NOC} = kN\pi d_c^2 C_{NO}$ (mol/s) [23]
$NO + CO \rightarrow \frac{1}{2}N_2 + CO_2$	$KT = 1.952 \times 10^{10} \exp\left(\frac{-19000}{T}\right)$ $k_1 = 0.1826,\ k_2 = 0.00786,\ k_3 = 0.002531$	$R_{NOCO} = KT\left(\frac{k_1C_{NO}(k_2C_{CO}+k_3)}{k_1C_{NO}+k_2C_{CO}+k_3}\right)$ $(mol/m^3\,s)$ [80]
$NH_3 + \frac{5}{4}O_2 \rightarrow NO + \frac{3}{2}H_2O$	$k = 2.73 \times 10^{14} \exp\left(\frac{-38160}{T}\right)$	$R_{NH_3NO} = kC_{NH_3}C_{O_2}$ $(mol/m^3\,s)$ [80]
$NH_3 + \frac{3}{4}O_2 \rightarrow \frac{1}{2}N_2 + \frac{3}{2}H_2O$	$k = 3.38 \times 10^7 \exp\left(\frac{-10000}{T}\right)$ $k' = 0.054$	$R_{NH_3N_2} = \frac{kC_{NH_3}C_{O_2}}{C_{O_2}+k'}$ $(mol/m^3\,s)$ [80]
$NO + NH_3 + \frac{1}{2}O_2 \rightarrow N_2 + \frac{3}{2}H_2O$	$k = 1.1 \times 10^{12} \exp\left(\frac{-27680}{T}\right)$	$R_{NONH_3} = k\sqrt{C_{O_2}}\sqrt{C_{NH_3}}\sqrt{C_{NO}}$ $(mol/m^3\,s)$ [80]
$CaO + SO_2 + \frac{1}{2}O_2 \rightarrow CaSO_4$	$k_L = \frac{\pi}{6}d_s^3 k_{vL}C_{SO_2}(1/s)$ [9,72,73]	$k_{vL} = 490 \exp\left(\frac{-17500}{R_gT}\right)S_g\lambda_s$ $(kg/m^2\,s)$ [28] $S_g = -384T + 5.6 \times 10^4 \quad T \geq 1253\,K$ $S_g = 35.9T - 3.67 \times 10^4 \quad T < 1253\,K$

formation is complex. NO_x formations in combustion processes result from a combination of a thermal generation process and fuel-nitrogen oxidation. At very high temperatures, thermal generation of NO_x from the air nitrogen becomes very important, while at low temperatures found in a CFBC, the dominant source of NO_x is fuel-nitrogen oxidation [18–20]. Typically, significant amounts of the fuel-nitrogen remain in the char after the devolatilization. The oxidation of this char-nitrogen gives an important contribution to the total nitrogen oxide emissions from the combustor. The mechanism of char-nitrogen oxidation to the products is very complex, and includes not only several homogeneous and heterogeneous reactions but also mass transfer effects inside the pore system of the char and in the boundary layer surrounding the particle [23]. In the present study, fuel-NO_x can be formed through: Combustion of the nitrogenous species released with volatile matter (such as HCN, NH_3), and oxidation of the nitrogen retained in the char. These reactions, resulting in rapid formation of NO_x, are most likely to proceed in the bottom zone. Meanwhile, in zones with volume O_2 concentrations lower than 10–12%, the NH_3 concentration is probably elevated due to the rapid formation of NH_3 from HCN [77] as well as because of the emission of NH_3 released with volatiles from fuel particles present in these zones. In the upper zone (with lower O_2 concentrations) this may lead to NO_x reduction through its reaction with NH_3, followed by formation of nitrogen gas and water vapor, i.e. neutral products. The alternative mechanisms of NO_x reduction in the upper zone involve reactions of NO_x with carbon and CO on the char surface [78,79] which are highly probable when firing high-ash fuels. The chemical reactions with their corresponding reaction rates for NO_x emissions formation and retention in the model are given in Table 1.

2.3. Heat transfer

In the model, the overall heat transfer coefficient from bed to wall at the bottom zone is calculated by Basu and Nag [81]. In the upper zone, based on the special hydrodynamics of the CFBC, the cluster renewal model of the bed to the wall heat transfer process has been described in the literature [1,80]. The dilute phase is comprised of a continuous upflowing gas phase with thinly dispersed solids and a relatively denser phase moving downward along the heat transfer surfaces. The contact resistance between adjacent materials is ignored. The heat transfer equations used in the model are given in Table 2. The structure and details of the heat transfer model have been given in a previous study [82].

3. Numerical solution

The model allows dividing the calculation domain into $m \times n$ control volumes, in the radial and the axial directions and in the core and the annulus regions, respectively. In this study the calculation domain is divided into 8×50 control volumes in the radial and the axial directions and in the core and the annulus regions, respectively. With the cylindrical system of coordinates, a symmetry boundary condition is assumed at the column axis. At the walls, a partial slip condition is assumed for the solid and the gas phases [83]. Tsuo and Gidaspow [83] had successfully applied the two-fluid model with effective solid viscosity based on a solid stress modulus to describe core annular flow behavior in a riser. For two-phase flow, two friction coefficients are obtained, one for the gas and one for the solid. Modified Hagen-Poiseuille expression is used for wall friction factor of gas phase and Konno's correlation is used for wall friction factor of solid phase in the model [34,44].

The set of differential equations governing mass, momentum and energy for the gas and solid phases are given in detail in a previous study [34] and are solved with a computer code developed by the author in FORTRAN language where the time step is 10^{-6} s. The Gauss–Seidel iteration which contains successful relaxation method and combined Relaxation Newton–Raphson methods are used for solving procedure. Details about solving procedure are given elsewhere [34].

Inputs for the model are combustor dimensions and construction specifications (insulation thickness and materials), primary and secondary air flow rates; coal feed rate and particle size

Table 2
Heat transfer equations used in the model

Bottom zone	
$h = 40(\rho_b)^{1/2}$ [81]	
$\rho_b = \rho(1-\varepsilon) + C\varepsilon$	
Upper zone	
$h = \varepsilon_p h_p + \varepsilon h_g + \varepsilon_p h_{r,p} + \varepsilon h_{r,g}$ [1,80]	
$h_p = \frac{k_g}{d_p}0.009 \times Pr^{0.33}Ar^{0.5}$	$h_{r,p} = \frac{\sigma(T_p^4 - T_{wall}^4)}{[(e_p^{-1} - e_{wall}^{-1})-1](T_p - T_{wall})}$
$h_g = \left(\frac{k_g}{d_p}\right)\left(\frac{c_p}{c_g}\right)\left(\frac{C}{\rho}\right)^{0.3}\left(\frac{U_{ter}}{gd_p}\right)^{0.21}Pr$	$h_{r,g} = \frac{\sigma(T_g^4 - T_{wall}^4)}{[(e_g^{-1} - e_{wall}^{-1})-1](T_g - T_{wall})}$

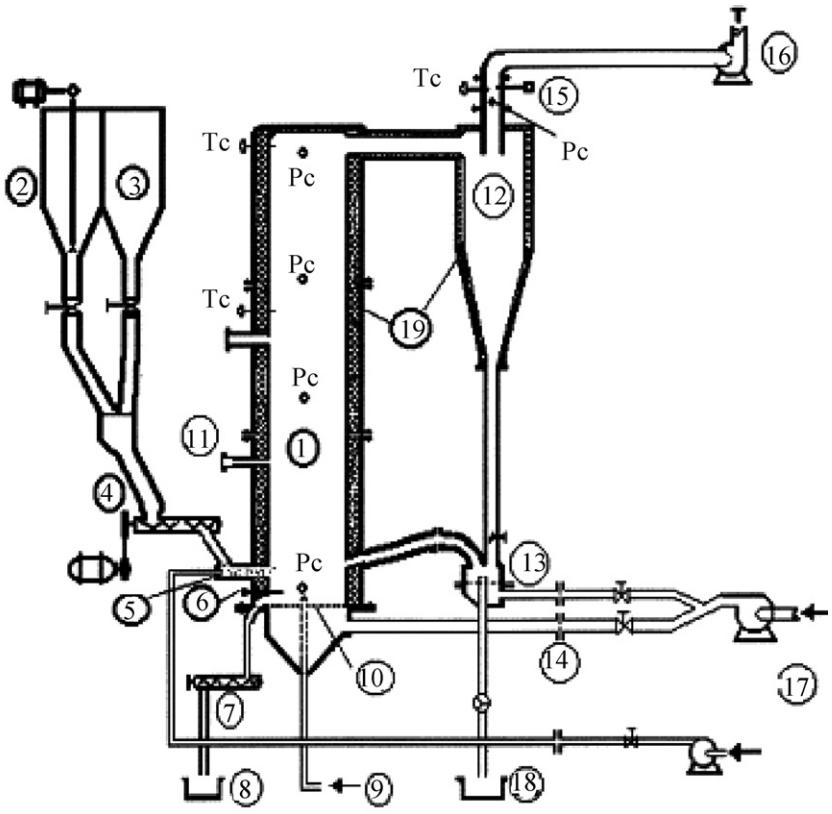

Fig. 3. Schematic diagram of the 50 kW pilot scale CFBC experimental setup [5].

distribution, coal properties, Ca/S ratio, limestone particle size distribution, inlet pressure and temperature, ambient temperature and the superficial velocity. The secondary air injection affects the concentration of oxygen, the bed voidage with increasing gas flow rate, the velocity profiles of the gas and the solid phases and the overall bed temperature. A continuity condition is used for the gas phase at the top of the cyclone. The cyclone is considered to have 98% collection efficiency. The solids circulation rate is computationally determined by the inlet pressure and the operational bed velocity (the superficial velocity). Simulation model calculates the axial and radial distribution of voidage, velocity, particle size distribution, pressure drop, gas emissions and temperature at each time interval for gas and solid phases both for dense bed and for riser. While investigating the effects of operational parameters, the mean bed temperature value is considered as 850 °C.

4. Comparison data

The comparison data are obtained from three different size CFBC, which use different kinds of low-grade Turkish lignites, the 50 kW pilot scale CFBC using Beypazari lignite, the 80 kW pilot scale CFBC using Tuncbilek lignite and industrial scale 160 MW CFBC using Can lignite (during the commissioning period). To test and validate the model presented in this paper, the same input variables in the tests are used as the simulation program input in the comparisons.

Schematic diagrams of pilot scale CFBCs has shown in Figs. 3 and 4. In the pilot scale CFBC of 50 kW the riser is a cylinder of 12.5 cm i.d. and 130 cm combustor height [5]. Particles leaving the combustor are collected by a cyclone and recycled back to the combustor by use of a fluidized bed feeding unit which has dimensions of 10 cm × 14 cm × 10 cm. LPG is used to preheat the bed material. Beypazari lignite, which is crushed and sieved to 900 μm average particle size, is fed to the combustor and its properties are shown in Table 3. Limestone sieved to 71–100 μm size is used as adsorbent. In the experiments 20% excess air is used. A more detailed description

Table 3
Proximate and ultimate analysis of lignites

	Beypazari lignite	Can lignite	Tuncbilek lignite
Proximate analysis (wt%)			
Moisture	12.40	21.40	20.80
Ash	38.34	30.40	23.70
Volatile matter	26.41	25.50	27.50
Fixed carbon	22.35	28.59	41.30
Ultimate analysis (wt%, dry)			
C	38.31	66.10	59.29
H	3.03	5.50	4.61
N	1.11	2.25	2.10
S	3.72	8.40	1.81
LHV (MJ/kg, dry)	10.283	11.704	22.083

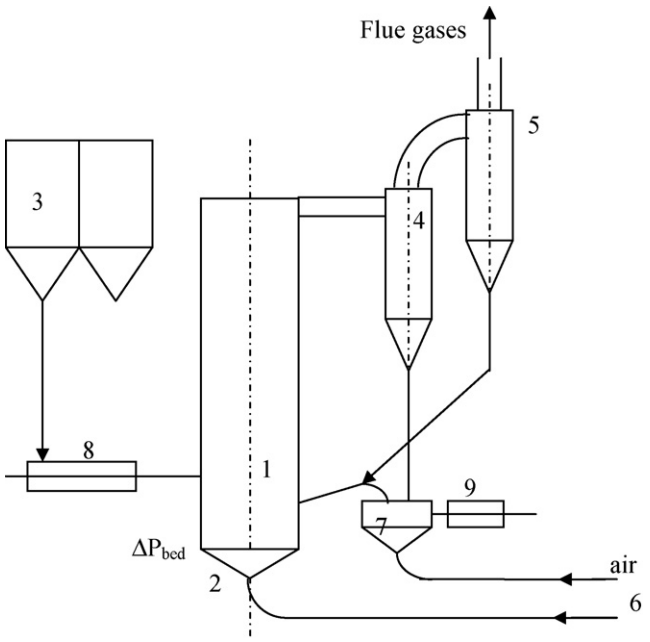

Fig. 4. Schematic diagram of the 80 kW pilot scale CFBC experimental setup [84,85].

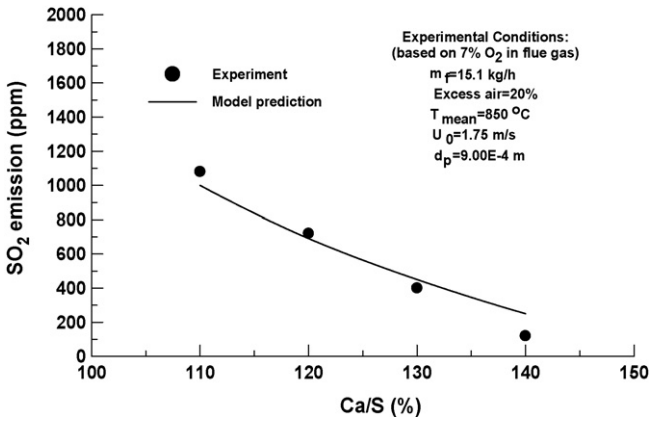

Fig. 5. Comparison of model SO_2 emission predictions with experimental data for 50 kW pilot scale CFBC [5] with regard to the Ca/S ratio (the uncertainty of m_f is 0.22% and SO_2 is 2.6 ppm).

of the experiment is given in Ozkan and Dogu [5]. The considered parameters and computation conditions are given in Table 4.

In the pilot scale CFBC of 80 kW the riser is a cylinder of 12.5 cm i.d. and has 180 cm combustor height [84]. The solid materials carried by combustion gases are returned to the main column by a re-circulation bed with the dimensions of 10 cm × 14 cm × 10 cm. The re-circulation bed is mounted with the main column at a level of 37 cm above its distributor plate. The air split ratio between the re-circulation bed and the riser is 1/5. Air from the re-circulation bed to the riser is not a secondary air. The secondary air inlets are located at 32 cm above the distributor. Natural gas is used to preheat the bed material. Tuncbilek lignite, which is crushed and sieved to 30–900 μm average particle size, is fed to the combustor and its properties are shown in Table 3. Limestone sieved to 71–100 μm size is used as adsorbent. Silica sand and ash were used as bed materials. The weighted average particle sizes are determined to be 56 μm for sand particles. A more detailed description of the experiment is given in Topal et al. [85]. The considered parameters and computation conditions are given in Table 4.

It must be noted that, the CFBCs used in the experiments mentioned above are small-scale pilot units. The operation velocity and the bed length of the system are designed to be 1.75 m/s and 1.80 m for 50 kW CFBC, and between 1.86 and 2.92 m/s and 1.80 m for 80 kW CFBC. However, in conventional CFBs these values are 5–8 m/s and 6 m or above. As a result of hydrodynamic experiments it is concluded that when operated at these values the system reaches the CFB regime and can be classified as a lower velocity CFB.

The industrial scale CFBC of 160 MW (Can Power Plant) has a combustor of 700 cm × 1400 cm square cross-section and 3700 cm height [43]. The combustor has a square cross-section, but the lower section has less cross-sectional area than the upper section. The technical parameters of the CFBC are steam capacity of 485 t h^{-1}, superheated steam temperature and pressure of 543 °C and 17.5 MPa, respectively. The secondary air ports are located at 500 cm from the distributor. Natural gas is used to preheat the bed material. The design fuel for the bed is Can lignite, which is crushed and sieved to 100–9000 μm average particle size, is fed to the combustor and its properties are shown in Table 3. Limestone sieved to 100–150 μm size is used as adsorbent. The operating parameters of data used for the comparison of CFB model is shown in Table 4.

5. Results and discussion

Fig. 5 presents the model predictions and experimental results of the effect of Ca/S ratio on SO_2 emission for 50 kW pilot scale CFBC. Detailed listing of the model input variables are given in Table 6. As can be seen in the figure, the SO_2 emission predictions are in good agreement with the experimental results for different Ca/S ratios. As the figure displays an increase in the Ca/S ratio gives a significant increase in the sulphur retention reached in the combustor. This phenomenon is also observed in the studies of Adanez et al. [9].

The increase of NO_x emissions with combustor temperature is observed in Fig. 6 for 50 kW pilot scale CFBC, whereas below 800 °C NO_x emissions are rather low. Over 800 °C some increase in NO_x emissions is observed. An increase in the combustor temperature increased the carbon combustion efficiency and decreased the carbon concentration due to the increase in the reaction rates. The

Table 4
Operating parameters of the experimental data referred to in this study

Operating parameters	50 kW pilot scale combustor [5]	80 kW pilot scale combustor [84,85]	160 MW industrial scale combustor [43]
Coal feed rate	15.1 kg/h	6–7.7 kg/h	110–120 t/h
Operation velocity (m/s)	1.75	3.60–9.23	4–6
Bed temperature (°C)	850–900	860–900	850–900
Primary/secondary air ratio	2/3	2/3	2/3
Bed area (m^2)	0.0122	0.0122	98
Size of coal feed (mm)	0.03–0.90	0.03–0.90	0.1–9.0
Mean size of sorbent feed (mm)	0.071–0.100	0.071–0.100	0.1–0.15

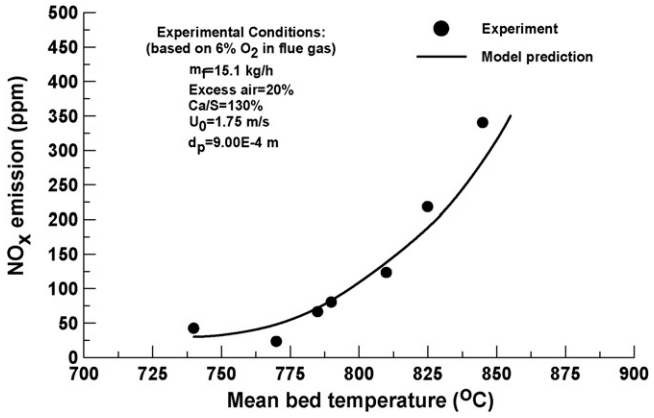

Fig. 6. Comparison of model NO_x emission predictions with experimental data for 50 kW pilot scale CFBC [5] with regard to the mean bed temperature (the uncertainty of m_f is 0.22% and NO_x is 1.6 ppm).

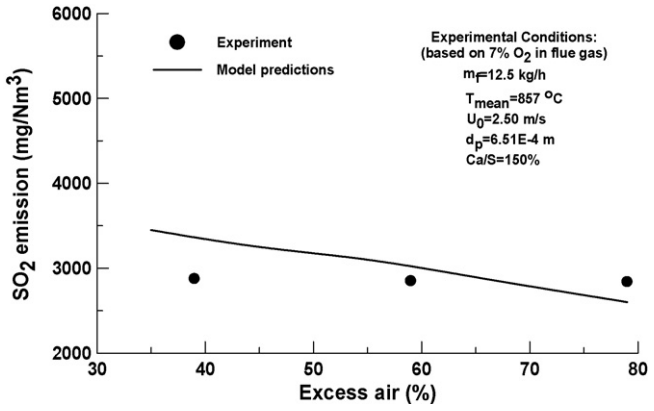

Fig. 7. Comparison of model SO_2 emission predictions with experimental data for 80 kW pilot scale CFBC [84,85] with regard to the excess ratio (the uncertainty of m_f is 0.18% and SO_2 is 3.6 mg/Nm^3).

reduction of NO_x emissions is proportional to the presence of char particles in the control volume and low char particle concentration causes the increase in NO_x emissions. On the other hand, these values are still much less than the values reported for conventional fluidized bed combustors [5,85]. It is clearly seen from Fig. 6 both experimental data and model predictions show the close agreement. Detailed listing of the model input variables are given in Table 6.

In Figs. 7 and 8, SO_2 and NO_x emissions based on 7% O_2 in the flue gas for 80 kW pilot scale CFBC are plotted with respect to excess air which ranges between 35% and 80%. Detailed listing of the model input variables are given in Table 6.

The general tendency is for a decrease on the efficiency of SO_2 removal by limestone with an increase in excess air [36]. This

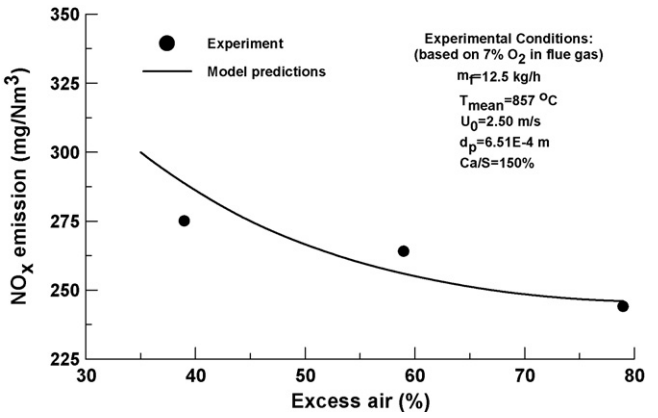

Fig. 8. Comparison of model NO_x emission predictions with experimental data for 80 kW pilot scale CFBC [84,85] with regard to the excess ratio (the uncertainty of m_f is 0.12% and NO_x is 1 mg/Nm^3).

phenomenon is explained by the fact that as the excess air value increases, the mean bed temperature decreases due to higher heat losses with increasing flue gas flow rates to the ambient. This causes the reaction rate of char combustion to decrease, which leads to limits the liberation of the fixed sulphur as SO_2. The same tendency is observed in model predictions (Fig. 7). In Fig. 8, the NO_x emission decreases with increasing excess air as observed in both experimental data and model predictions. Although the amount of oxygen increases with increasing excess air, decreasing bed temperature causes a negative effect on coal combustion efficiency which results in lower levels of NO_x formation [86,87]. Decreasing combustion efficiency also causes higher carbon content in the combustor. Thus the reduction rate of NO_x increases (Fig. 8). Another explanation of decreasing SO_2 and NO_x emissions is the gas dilution caused by increasing excess air.

For the 160 MW industrial scale CFBC, temperature, SO_2 and NO_x emissions response in flue gases simulation and test results at the riser exit are compared at different coal feed rates and the results are presented in Table 5. Detailed listing of the model input variables are given in Table 6. It is seen that the simulation results are in good agreement with industrial scale CFBC data as well.

Model predictions are in good agreement with both industrial and small-scale CFBCs which is an indication that the model is flexible enough to be used in different CFB applications and simulates under a wide range of operating conditions such as coal type, combustor temperature, excess air ratio and Ca/S ratio. Moreover, both experimental data and model predictions show the close agreement and have low and acceptable levels of gaseous emissions.

6. Effects of operational parameters

In the present study, the variations of the overall SO_2 and NO_x emissions under different operational conditions such as excess

Table 5
Comparison of simulation results with 160 MW industrial CFBC test results [43]

Time (min)	Coal feed (t/h)	T (°C)		Err.	NO_x (mg/Nm^3)		Err.	SO_2 (mg/Nm^3)		Err.
		Model	Data	(%)	Model	Data	(%)	Model	Data	(%)
30	119.1	798.50	807.1	1.06	97.90	97.1	0.82	1290.55	1290.9	0.020
60	119.0	798.79	809.1	1.27	96.90	95.9	1.03	1274.08	1272.4	0.130
90	116.9	800.36	812.4	1.48	97.56	98.7	1.14	1183.50	1184.9	0.110
120	116.3	798.59	814.9	2.00	92.52	92.7	0.18	1235.86	1235.5	0.020
150	116.0	798.40	812.3	1.71	102.03	102.5	0.45	1185.11	1184.9	0.010
180	118.4	798.26	805.5	0.89	98.95	98.7	0.29	1205.80	1204.0	0.140
210	113.8	804.01	809.3	0.65	99.06	98.2	0.87	1240.32	1240.2	0.009

Table 6
Model input variables

Comparison element	D (m)	H_b (m)	Inlet pressure (atm)	Excess air (%)	Superficial velocity (m/s)	Coal feed rate (kg/h)	Mean coal particle size (μm)	Mean bed temperature (°C)	Ca/S	Mean sorbent particle size (μm)
50 kW CFBC										
SO_2	0.125	1.3	1.12	20	1.75	15.1	900	850	1.1–1.4	71
NO_x	0.125	1.3	1.12	20	1.75	15.1	900	740–855	1.3	71
80 kW CFBC										
SO_2	0.125	1.8	1.12	35–80	2.50	12.5	651	857	1.5	71
NO_x	0.125	1.8	1.12	35–80	2.50	12.5	651	857	1.5	71
160 MW CFBC										
SO_2	0.125	1.8	1.12	20–40	6.70	113.8–119.1	6500	800	1.5	71
NO_x	0.125	1.8	1.12	20–40	6.70	113.8–119.1	6500	800	1.5	71

air (20–100%), bed operational velocity (4.15–6.50 m/s), coal particle diameter (540–852 μm) and inlet bed pressure (1.6–2.2 atm) are analyzed for the 80 kW pilot scale CFBC conditions with the developed and validated 2D model with respect to these emissions.

Fig. 9 shows the effects of excess air and coal particle diameter on the overall SO_2 emission in modeling results. Fig. 9 plots the predicted model results for three particle diameters (540, 600 and 750 μm) and for five excess air ratios (of about 20%, 40%, 60%, 80% and 100%). For this assumption inlet bed pressure is 1.2 atm and coal feed rate is 7.20 kg/h. The SO_2 generation rate from the char depends on its combustion rate, which depends on the temperature, excess air, O_2 concentration, etc. [72]. Although the amount of oxygen increases with increasing excess air, decreasing bed temperature causes a negative effect on coal combustion efficiency and limits the liberation of the fixed sulphur as SO_2. Fig. 9 shows the decrease of SO_2 emission with increasing excess air which is also observed in the comparison of model predictions with experimental results given above (Fig. 5). Although the general tendency is for a decrease in the SO_2 emission as excess air increases, it is observed that the effect of excess air on the overall SO_2 emission is not significant. Another explanation of decreasing SO_2 emission is the gas dilution caused by increasing excess air. The decrease of SO_2 emission with increasing particle size may be explained as being a consequence of the longer SO_2 diffusion parts in larger particles.

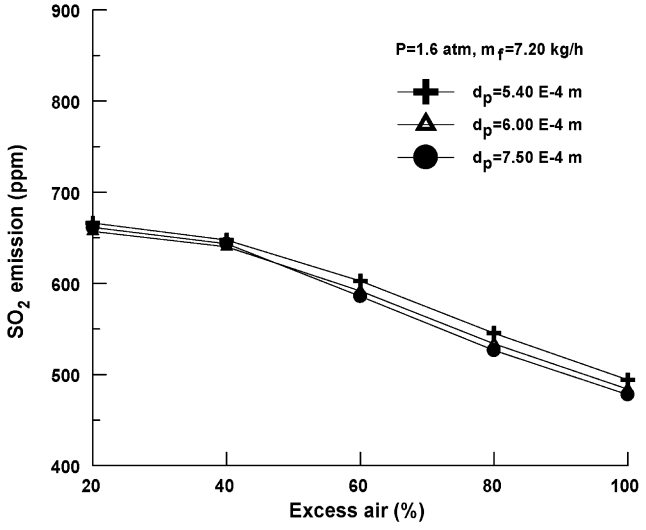

Fig. 9. Effect of excess air ratio on the overall SO_2 emission from the combustor.

Fig. 10 shows the effects of bed operational velocity and coal particle diameter on the overall SO_2 emission in modeling results. Fig. 10 plots the predicted model results for three particle diameters (540, 651 and 852 μm) and for six bed operational velocity values (of about 4.15, 4.50, 5.00, 5.50, 6.00 and 6.50 m/s). For this assumption inlet bed pressure is 1.6 atm and coal feed rate is 7.20 kg/h. The bed operational velocity in the combustor is one of the basic design variables of the process. The reason is that with the increase of bed operating velocity the hydrodynamic condition of the combustor

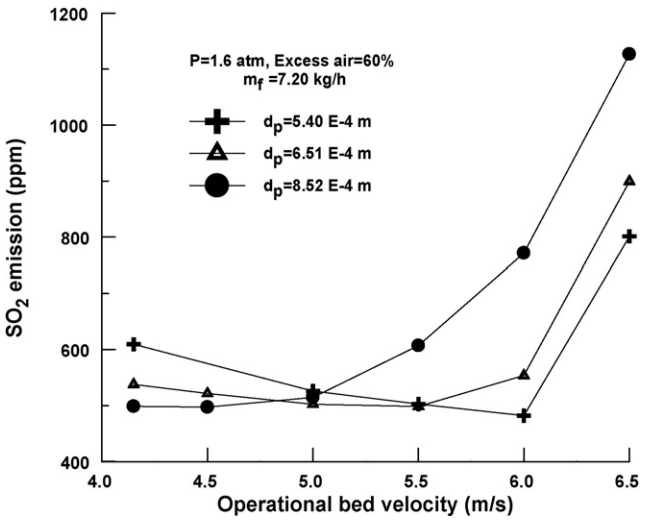

Fig. 10. Effect of operational bed velocity on the overall SO_2 emissions from the combustor.

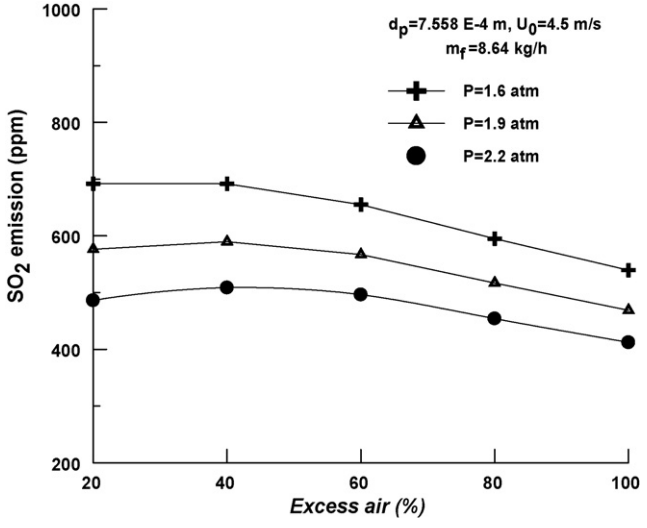

Fig. 11. Effect of excess air ratio and inlet bed pressure on the overall SO_2 emissions from the combustor.

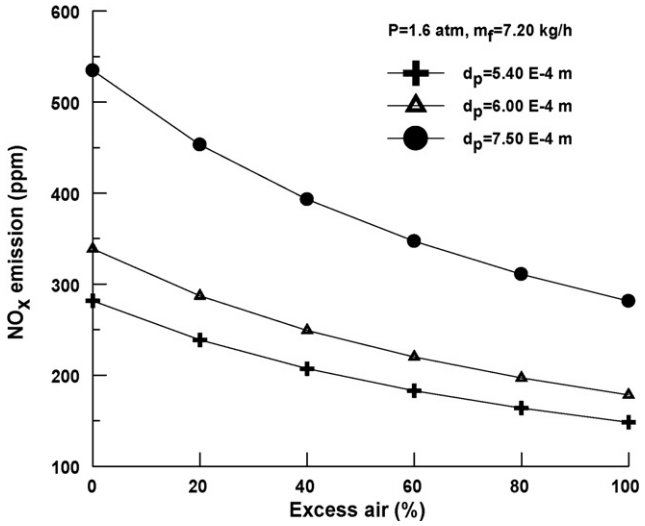

Fig. 12. Effect of excess air ratio on the overall NO_x emission from the combustor.

changes. In Fig. 10, it is observed that SO_2 emission decreases with increasing the operational velocity which causes a decrease in the residence time of particles and so its combustion rates. This effect is reversed after the value of 5 m/s (Fig. 10). As can be seen in the figure, a further increase in the velocity decreases sulphur retention mainly due to two effects. Firstly, it increases the coal throughput increasing the SO_2 generation and secondly, it increases circulation flow rates of solids and thus decreases the mean residence time of limestone particles and their conversion in the bed. Besides, particle residence time decreases with decreasing coal particle size and causes lower SO_2 emission formation if other parameters are kept unchanged.

Fig. 11 shows the effects of excess air and inlet bed pressure value on the overall SO_2 emission in modeling results. Fig. 11 plots the predicted model results for three inlet bed pressure values (1.6, 1.9 and 2.2 atm) and for five excess air ratios (of about 20%, 40%, 60%, 80% and 100%). For this assumption coal particle diameter is 755.8 μm, bed operational velocity is 4.5 m/s and coal feed rate is 8.64 kg/h.

As the inlet bed pressure value increases turbulence dissipation effect in the combustor, combustion in the bed becomes more

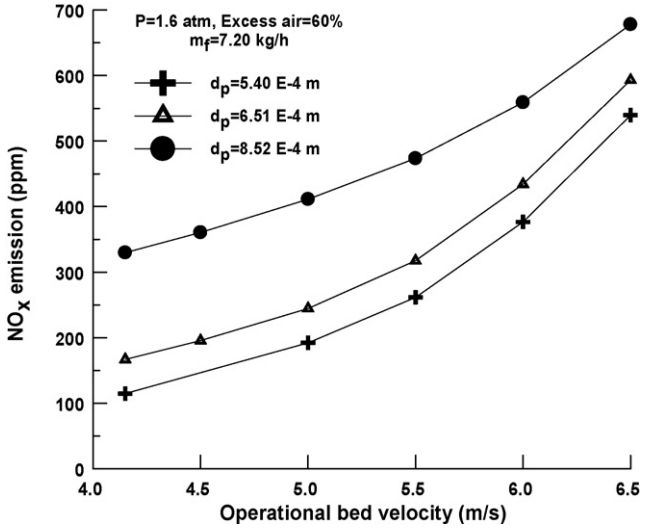

Fig. 13. Effect of operational bed velocity on the overall NO_x emission from the combustor.

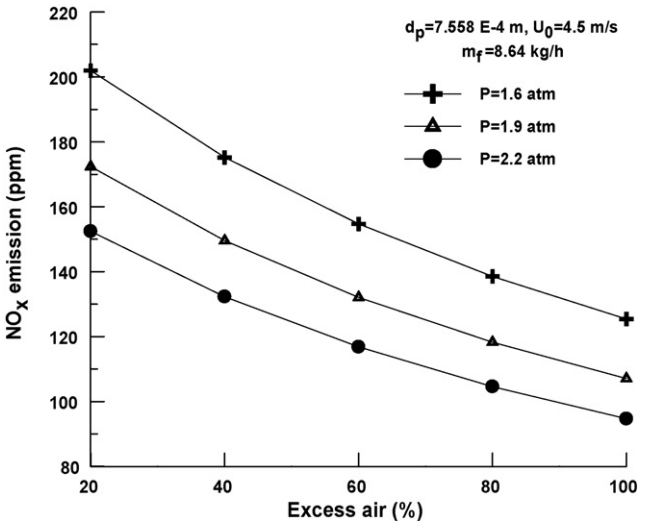

Fig. 14. Effect of excess air ratio and inlet bed pressure on the overall NO_x emission from the combustor.

effective which results higher mean bed temperature and lower CO emission values in flue gases (Fig. 11). It is observed that inlet bed pressure value has positive effect on SO_2 emission. Fig. 11 shows the decrease of SO_2 emission with increasing inlet bed pressure value if other parameters are kept unchanged. A bigger inlet bed pressure value will result in lower emission of SO_2 as clearly seen from Fig. 11. This is due to the turbulence dissipation effect which increases with increasing inlet bed pressure value and causes a positive effect on the mixing conditions.

As it is seen from Fig. 12, the NO_x emission profile tends to follow the same trend as the SO_2 emission profile. Increasing excess air results in lower levels of NO_x formation which is generated due to combustion efficiency decrease caused by lower bed temperature. Decreasing combustion efficiency also causes higher carbon content in the combustor. Thus the reduction rate of NO_x increases (Fig. 12). However, the effect of the excess air on the NO_x emission is more significant than to SO_2 emission.

As the operational velocity increases particle residence time in the combustor, char combustion rate and bed temperature decreases which results higher CO emission values in flue gases. Suspension density in the bed decreases with increasing superficial velocity. So, the contact time of NO_x with char particle is reduced, thus reducing the rate of reduction of NO_x. Therefore, NO_x emissions increase with the superficial velocity of the combustor (Fig. 13). The high fuel-N contents of the large size of particles causes the high rates of NO_x emission formation as it is clearly seen from Figs. 12 and 13.

Fig. 14 shows the decrease of the NO_x emission with increasing inlet bed pressure value. It is also observed that inlet bed pressure value has positive effect on the NO_x emission due to the fact that increasing inlet bed pressure value causes stronger turbulence in the combustor which results in better mixing of particulate solids and gases. The inlet bed pressure value has a more significant effect on NO_x emission than to excess air ratio. A bigger inlet bed pressure value will result in lower emission NO_x as it is the case with SO_2 if other parameters are kept unchanged as clearly seen from Fig. 14.

7. Conclusions

SO_2 and NO_x emissions are two major air pollutants released from a fossil fuel fired combustor. Using CFB combustion technology can decrease these pollutant gases in the production of energy.

Based on previous work on dynamic 2D coal combustion modeling of CFBCs, a modeling study of these pollutant emissions resulting from coal combustion in CFBCs is present in this study. Using this model, overall SO_2 and NO_x emissions are predicted for the combustion of three different kinds of low-grade Turkish lignites.

The variations of the overall SO_2 and NO_x emissions under different operational conditions such as excess air (20–100%), bed operational velocity (4.15–6.50 m/s), coal particle diameter (540–852 μm) and inlet bed pressure (1.6–2.2 atm) are analyzed with the developed and validated 2D model with respect to these emissions. As a result of this investigation, the general tendency is for a decrease in the SO_2 and NO_x emissions as excess air increases. The effect of the excess air on the NO_x emission is more significant than to SO_2 emission. NO_x emission increases with the operational bed velocity while SO_2 emission decreases. The inlet bed pressure value has positive effect on SO_2 and NO_x emissions. A bigger inlet bed pressure value will result in lower emissions of SO_2 and NO_x if other parameters are kept unchanged. The inlet bed pressure value has a more significant effect on NO_x emission than to excess air ratio.

The present study proves that CFB combustion allows clean and efficient combustion of low-grade coal which is demonstrated by the fact that both experimental data and model predictions have low and acceptable level of SO_2 and NO_x emissions.

References

[1] P. Basu, Combustion of coal in circulating fluidized-bed boilers: a review, Chemical Engineering Science 54 (1999) 5547–5557.
[2] L. Reh, Development potentials and research needs in circulating fluidized bed combustion, China Particuology 1 (5) (2003) 185–200.
[3] A. Gungor, Analysis of combustion efficiency in CFB coal combustors, Fuel 87 (7) (2008) 1083–1095.
[4] A. Bosoaga, N. Panoiu, L. Mihaescu, R.I. Backreedy, L. Ma, M. Pourkashanian, A. Williams, The combustion of pulverised low grade lignite, Fuel 85 (10–11) (2006) 1591–1598.
[5] G. Ozkan, G. Dogu, Combustion of a high ash and sulfur containing lignite in a pilot circulating fluidized bed combustor and its pollution characteristics, Chemical Engineering and Processing 41 (1) (2002) 11–15.
[6] I. Heinbockel, F.N. Fett, Simulation of a combined cycle power based on a pressurized circulating fluidized bed combustor, in: P. Basu (Ed.), Heat Recovery System & CHP, vol. 15, n. 2, Pergamon Press, Oxford, 1995, pp. 171–178.
[7] C.G. Remberg, A. Nemet, F.N. Fett, Towards a more general process model for power plants with atmospheric or pressurized fluidized bed combustion, in: F.D.S. Preto (Ed.), Proceedings of the 14th International Conference on Fluidized Bed Combustion, vol. 2, ASME, New York, 1997, pp. 1139–1149.
[8] L. Huilin, Z. Guangbo, B. Rushan, C. Yongjin, D. Gidaspow, A coal combustion model for circulating fluidized bed boilers, Fuel 79 (2000) 165–172.
[9] J. Adanez, P. Gayán, G. Grasa, L.F. de Diego, L. Armesto, A. Cabanillas, Circulating fluidized bed combustion in the turbulent regime: modeling of carbon combustion efficiency and sulfur retention, Fuel 80 (2001) 1405–1414.
[10] Q. Wang, Z. Luo, M. Ni, K. Cen, Particle population balance model for a circulating fluidized bed boiler, Chemical Engineering Journal 93 (2003) 121–133.
[11] Y. Hua, G. Flamant, J. Lu, D. Gauthier, Modelling of axial and radial solid segregation in a CFB boiler, Chemical Engineering and Processing 43 (8) (2003) 971–978.
[12] Y.H. Zhou, H.L. Lu, Y.R. He, Numerical prediction of combustion of carbon particle clusters in a circulating fluidized bed riser, Chemical Engineering Journal 118 (1–2) (2006) 1–10.
[13] T. Knoebig, K. Luecke, J. Werther, Mixing and reaction in the circulating fluidized bed—a three-dimensional combustor model, Chemical Engineering Science 54 (1999) 2151–2160.
[14] T. Hyppanen, Y.Y. Lee, A. Rainio, A three dimensional model for circulating fluidized bed combustion, in: P. Basu, M. Horio, M. Hasatani (Eds.), Circulating Fluidized Bed Technology III, Pergamon Press, Oxford, 1991, pp. 563–568.
[15] Y.P. Tsuo, Y.Y. Lee, A. Rainio, T. Hyppanen, Study of SO_2/NO_2/N_2O emission from CFB boilers with a three-dimensional CFB combustion model, in: M. Kwauk, J. Li (Eds.), Circulating Fluidized Bed Technology V, Science Press, Beijing, 1997, pp. 466–481.
[16] L. Reh, Challenges of circulating fluid-bed reactors in energy and raw materials industries, Chemical Engineering Science 54 (22) (1999) 5359–5368.
[17] I. Aarna, E.M. Suuberg, The role of carbon monoxide in the NO–carbon reaction, Energy & Fuels 13 (1999) 1145–1153.
[18] I. Aarna, E.M. Suuberg, A review of the kinetics of the nitric oxide–carbon reaction, Fuel 76 (1997) 475–482.
[19] Y.H. Li, G.Q. Lu, V. Rudolph, The kinetics of NO and N_2O reduction over coal chars in fluidized bed combustion, Chemical Engineering Science 53 (1998) 1–7.
[20] H. Aoki, A. Suzuki, Y. Hisaeda, Y. Suwa, T. Nakagawa, M. Yaga, M. Shoji, T. Miura, Recent research and development of combustion simulation, Heat Transfer Asian Research 30 (7) (2001) 581–612.
[21] I.M. Bews, A.N. Hayhurst, S.M. Richardson, S.G. Taylor, The order, Arrhenius parameters, and mechanism of the reaction between gaseous oxygen and solid carbon, Combustion and Flame 124 (2001) 231–245.
[22] R. Abe, H. Sasatsu, T. Harada, N. Misawa, I. Saitou, Prediction of emission gas concentration from pressurized fluidized bed combustion (PFBC) of coal under dynamic operation conditions, Fuel 80 (2001) 135–144.
[23] P. Kilpinen, S. Kallio, J. Konttinen, V. Barisic, Char-nitrogen oxidation under fluidised bed combustion conditions: single particle studies, Fuel 81 (2002) 2349–2362.
[24] H. Liu, B. Feng, J.D. Lu, Coal property effects on N_2O and NO_x formation from circulating fluidized bed combustion of coal, Chemical Engineering Communications 192 (10–12) (2005) 1482–1489.
[25] Y. Zhao, P.Y. Xu, D. Fu, Experimental study on simultaneous desulfurization and denitrification based on highly active absorbent, Journal of Environmental Sciences-China 18 (2) (2006) 281–286.
[26] F. Winter, Single Fuel Particle and NO_x/N_2O-Emission Characteristics Under Circulating Fluidized Bed Combustor Conditions, Ph.D. Thesis, University of Technology, Vienna, Austria, 1995.
[27] M. Stenseng, W. Lin, J.E. Johnsson, K.D. Johansen, Modeling of devolatilization in CFB combustion, in: F.D.S. Preto (Ed.), Proceedings of the 14th International Conference on Fluidized Bed Combustion, vol. 1, ASME, New York, 1997, pp. 117–124.
[28] P. Kilpinen, P. Glarborg, M. Hupa, Reburning chemistry at fluidized bed combustion conditions-a kinetic modeling study, Industrial Engineering and Chemistry Research 31 (1992) 1477–1490.
[29] J. Talukdar, P. Basu, A simplified model of nitric oxide emission from a circulating fluidized bed combustor, The Canadian Journal of Chemical Engineering 73 (1995) 635–643.
[30] S. Goel, A. Sarofim, P. Kilpinen, M. Hupa, Emissions of nitrogen oxides from circulating fluidized bed combustors: modeling results using detailed chemistry, in: Proceedings of the 26th International Symposium on Combustion, The Combustion Institute, Naples, 1996.
[31] D. Barletta, A. Marzocchella, P. Salatino, Modelling the SO_2–limestone reaction under periodically changing oxidizing/reducing conditions: the influence of cycle time on reaction rate, Chemical Engineering Science 57 (2002) 631–641.
[32] M.J. Fernandez, H. Kasman, A. Lyngfelt, Methods for measuring the concentrations of SO_2 and gaseous reduced sulphur compouds in the combustion chamber of a circulating fluidized bed boiler, The Canadian Journal of Chemical Engineering 78 (2000) 1138–1144.
[33] A. Gungor, N. Eskin, Analysis of environmental benefits of CFB combustors via one-dimensional model, Chemical Engineering Journal 131 (1–3) (2007) 301–317.
[34] A. Gungor, N. Eskin, Two dimensional coal combustion modeling of CFB, International Journal of Thermal Sciences 47 (2008) 157–174.
[35] M. Ilic, B. Grubor, V. Manovic, Sulfur retention by ash during coal combustion. Part I. A model of char particle combustion, Journal of the Serbian Chemical Society 68 (2003) 137–145.
[36] L.A.C. Tarelho, M.A.A. Matos, F.J.M.A. Pereira, The influence of operational parameters on SO_2 removal by limestone during fluidized bed coal combustion, Fuel Processing Technology 86 (2005) 1385–1401.
[37] V. Manovica, B. Gruborb, D. Loncarevicc, Modeling of inherent SO_2 capture in coal particles during combustion in fluidized bed, Chemical Engineering Science 61 (2006) 1676–1685.
[38] P. Basu, A. Sett, E.A.M. Gbordzoe, A simplified model for combustion of carbon in a circulating fluidized bed combustor, in: J.P. Mustonen (Ed.), Proceedings of the 9th International Conference on Fluidized Bed Combustion, ASME, New York, 1987, pp. 738–742.
[39] A. Svensson, F. Johnsson, B. Leckner, Fluid-dynamics of the bottom bed of circulating fluidized bed boilers, in: Proceedings of the 12th International Conference on Fluidized Bed Combustion, San Diego, CA, 1993, pp. 887–897.
[40] J. Werther, J. Wein, Expansion behavior of gas fluidized beds in the turbulent regime, AIChE Symposium Series 301 (90) (1994) 31–44.
[41] B. Leckner, M.R. Golriz, W. Zhang, B.A. Andersson, F. Johnsson, Boundary layers first measurement in the 12 MW CFB plant at Chalmers University, in: Proceedings of the 11th International Conference on Fluidized Bed Combustion, ASME, 1991, pp. 771–776.
[42] D. Montat, T.D. Maggio, 1D two-phase description of the thermal hydraulic behavior of the furnace of E. Huchet 125 MWe CFB boiler, in: Proceedings of the 5th International Conference on CFB, MSR6, Beijing, 1996.
[43] A. Gungor, Modeling of Circulating Fluidized Bed Combustors, Ph.D. Thesis, Istanbul Technical University Institute of Science and Technology, Turkey, 2006.
[44] A. Gungor, N. Eskin, Hydrodynamic modeling of a circulating fluidized bed, Powder Technology 172 (2007) 1–13.
[45] G. Palchonock, C. Breitholtz, H. Thunman, B. Leckner, Impact of heat and mass transfer on combustion of a fuel particle in CFB boiler, in: F.D.S. Preto (Ed.), Proceedings of the 14th International Conference on Fluidized Bed Combustion, ASME, New York, 1997, pp. 871–878.
[46] L. Huilin, B. Ruhsan, Y. Lidan, Z. Guangbo, T. Xiu, Numerical computation of a circulating fluidized bed combustor, International Journal of Energy Research 22 (1998) 1351–1364.

[47] P. Schlichthaerle, J. Werther, Axial pressure profiles and solids concentration distributions in the CFB bottom zone, Chemical Engineering Science 54 (1999) 5485–5493.
[48] M. Horio, Hydrodynamics, in: J.R. Grace, A.A. Avidan, T.M. Knowlton (Eds.), Circulating Fluidized Beds, Blackie Academic & Professional, London, 1992, 40 pp.
[49] S. Mori, C.Y. Wen, Estimation of bubble diameter in gaseous fluidized beds, AIChE Journal 21 (1975) 109–117.
[50] C.Y. Wen, Y.H. Yu, Mechanics of fluidization, Chemical Engineering Progress Symposium Series 62 (1966) 100–110.
[51] R.R. Rajan, C.Y. Wen, A comprehensive model for fluidized bed coal combustors, AIChE Journal 26 (1980) 642–655.
[52] K. Smolders, J. Baeyens, Hydrodynamic modelling of the axial density profile in the riser of a low-density circulating fluidized bed, The Canadian Journal of Chemical Engineering 79 (2001) 422–429.
[53] M.J. Rhodes, X.S. Wang, H. Cheng, T. Hirama, Similar profiles of solids flux in circulating fluidized bed risers, Chemical Engineering Science 47 (7) (1992) 1635–1643.
[54] C.A. Palmer, E. Tuncali, K.O. Dennen, T.C. Coburn, R.B. Finkelman, Characterization of Turkish coals: a nationwide perspective, International Journal of Coal Geology 60 (2–4) (2004) 85–115.
[55] A. Kucuk, Y. Kadioglu, M.S. Gulaboglu, A study of spontaneous combustion characteristics of a Turkish lignite: particle size, moisture of coal, humidity of air, Combustion and Flame 133 (3) (2003) 255–261.
[56] S. Cetinkaya, Y. Yurum, Oxidative pyrolysis of Turkish lignites in air up to 500 °C, Fuel Processing Technology 67 (3) (2000) 177–189.
[57] R. Loison, R. Chauvin, Pyrolyse rapide du charbon, Chemie et Industrie 91 (1964) 269–274.
[58] J. Hannes, U. Renz, C.M. Van den Bleek, The IEA model for circulating fluidized bed combustion, in: K.J. Heinschel (Ed.), Proceedings of the 13th International Conference on Fluidized Bed Combustion, ASME, Orlando, 1995, pp. 287–296.
[59] F. Bellgardt, F. Hembach, M. Schossler, J. Werther, Modeling of large scale atmospheric fluidized bed combustors, in: J.P. Mustonen (Ed.), Proceedings of the 9th International Conference on Fluidized Bed Combustion, ASME, Boston, 1987, 713 pp.
[60] Q. Wang, Z. Luo, X. Li, M. Fang, M. Ni, K. Cen, A mathematical model for a circulating fluidized bed (CFB) boiler, Energy 24 (1999) 633–653.
[61] H. Thunman, Loading and Size Distribution of Fuel in a Fluidized Bed Combustor, Master Thesis, Chalmers University of Technology, Goteborg, Sweden, 1997.
[62] E.A. Bramer, Flue gas emissions from fluidized bed combustion, in: M. Valk (Ed.), Atmospheric Fluidized Bed Coal Combustion, Research, Development and Application, Elsevier, The Netherlands, 1995, p. 51.
[63] D.W. Marsh, D.L. Ulriehson, Rate and diffusional study of the reaction of calcium oxide with sulfur dioxide, Chemical Engineering Science 40 (1985) 423–433.
[64] S. Lalvani, M. Pata, R.W. Coughlin, Sulphur removal from coal by electrolysis, Fuel 62 (4) (1983) 427–437.
[65] K. Laursen, J.R. Grace, Some implications of co-combustion of biomass and coal in a fluidized bed boiler, Fuel Processing Technology 76 (2) (2002) 77–89.
[66] K. Dam-Johansen, P.F.B. Hansen, K. Ostergaard, High-temperature reaction between sulphur dioxide and limestone. III. A grain-micrograin model and its verification, Chemical Engineering Science 46 (1991) 847–853.
[67] K. Laursen, J.R. Grace, C.J. Lim, Enhancement of the sulfur capture capacity of limestones by the addition of Na_2CO_3 and NaCl, Environmental Science and Technology 35 (21) (2001) 4384–4389.
[68] K. Dam-Johansen, Svovldiozid Binding paa Toerkalk, Ph.D. Thesis, Technical University of Denmark, 1987.
[69] B. Leckner, L.E. Amand, Emission from a circulating and a stationery fluidized bed boiler a comparison, in: J.P. Mustonen (Ed.), Proceedings of the 9th International Conference on Fluidized Bed Combustion, ASME, Boston, 1987, pp. 891–897.
[70] E.D. Ducarne, J.C. Dolignier, E. Marty, G. Martin, L. Delfosse, Modelling of gaseous pollutants emissions in circulating fluidized bed combustion of municipal refuse, Fuel 77 (13) (1998) 1399–1410.
[71] J. Talukdar, P. Basu, J.H. Greenblatt, Reduction of calcium sulfate in a coal-fired circulating fluidized bed furnace, Fuel 75 (9) (1996) 1115–2112.
[72] J. Adanez, L.F. de Diego, P. Gayan, L. Armesto, A. Cabanillas, Modeling of sulfur retention in circulating fluidized bed combustors, Fuel 75 (3) (1996) 262–270.
[73] R.H. Borgwardt, Kinetics of the reaction of SO_2 with calcined limestone, Environmental Science and Technology 4 (1970) 49–57.
[74] T. Furusawa, T. Honda, J. Tatano, D.J. Kunii, Abatement of nitric oxide emission in fluidized bed combustion of coal, Journal of Chemical Engineering of Japan 11 (5) (1978) 377–383.
[75] J. Zhao, C. Brereto, J.R. Grace, C.J. Lim, R. Legros, Gas concentration profiles and NO_x formation in circulating fluidized bed combustion, Fuel 76 (9) (1997) 853–860.
[76] L. Plass, H. Bierbach, P. Gummel, Lurgi GmbH Gervinusstraße, KW0208a, Frankfurt, 1986.
[77] F. Winter, C. Wartha, H. Hofbauer, NO and N_2O formation during the combustion of wood, straw, malt waste and peat, Bioresource Technology 70 (1) (1999) 39–49.
[78] B. Leckner, M. Karlsson, Gaseous emissions from circulating fluidized bed combustion of wood, Biomass and Bioenergy 4 (5) (1993) 379–389.
[79] J. Werther, M. Saenger, E.-U. Hartge, T. Ogada, Z. Siagi, Combustion of agricultural residues, Progress in Energy and Combustion Science 26 (1) (2000) 1–27.
[80] E.D. Ducarne, J.C. Dolignier, E. Marty, G. Martin, L. Delfosse, Modelling of gaseous pollutants emissions in circulating fluidized bed combustion of municipal refuse, Fuel 77 (1998) 1399–1410.
[81] P. Basu, P.K. Nag, Review of heat transfer in high temperature circulating fluidized bed, Chemical Engineering Science 51 (1996) 1–26.
[82] A. Gungor, N. Eskin, Effects of immersed surfaces on the combustor efficiency of small-scale fluidized beds, International Journal of Applied Thermodynamics 8 (3) (2005) 127–136.
[83] Y.P. Tsuo, D. Gidaspow, Computation of flow patterns in circulating fluidized beds, AIChE Journal 36 (6) (1990) 885–896.
[84] H. Topal, Experimental Investigation of the Hydrodynamic, Combustion and Emission Properties of a Circulating Fluidized Bed, Ph.D. Thesis, Gazi University Institute of Science and Technology, Turkey, 1999.
[85] H. Topal, A.T. Atimtay, A. Durmaz, Olive cake combustion in a circulating fluidized bed, Fuel 82 (2004) 1049–1056.
[86] W. Permchart, V.I. Kouprianov, Emission performance and combustion efficiency of a conical fluidized-bed combustor firing various biomass fuels, Bioresource Technology 92 (1) (2004) 83–91.
[87] T. Madhiyanon, A. Lapirattanakun, P. Sathitruangsak, S. Soponronnarit, A novel cyclonic fluidized-bed combustor (ψ-FBC): combustion and thermal efficiency, temperature distributions, combustion intensity, and emission of pollutants, Combustion and Flame 146 (1–2) (2006) 232–245.